Efficacy Evaluation of SAVE for the Diagnosis of Superficial Neoplastic Lesion

**FARAH DEEBA, (Student Member, IEEE), SHAHED K. MOHAMMED, (Student Member, IEEE),
FRANCIS MINHTHANG BUI, (Member, IEEE), AND KHAN A. WAHID, (Senior Member, IEEE)**

University of Saskatchewan, Saskatoon, SK S7N5A9, Canada

CORRESPONDING AUTHOR: F. DEEBA (farah.deeba@usask.ca)

ABSTRACT The detection of non-polypoid superficial neoplastic lesions using current standard of white light endoscopy surveillance and random biopsy is associated with high miss rate. The subtle changes in mucosa caused by the flat and depressed neoplasms often go undetected and do not qualify for further investigation, e.g., biopsy and resection, thus increasing the risk of cancer advancement. This paper presents a screening tool named the saliency-aided visual enhancement (SAVE) method, with an objective of highlighting abnormalities in endoscopic images to detect early lesions. SAVE is a hybrid system combining image enhancement and saliency detection. The method provides both qualitative enhancement and quantitative suspicion index for endoscopic image regions. A study to evaluate the efficacy of SAVE to localize superficial neoplastic lesion was performed. Experimental results for average overlap index >0.7 indicated that SAVE was successful to localize the lesion areas. The area under the receiver-operating characteristic curve obtained for SAVE was 94.91%. A very high sensitivity (100%) was achieved with a moderate specificity (65.45%). Visual inspection showed a comparable performance of SAVE with chromoendoscopy to highlight mucosal irregularities. This paper suggests that SAVE could be a potential screening tool that can substitute the application of burdensome chromoendoscopy technique. SAVE method, as a simple, easy-to-use, highly sensitive, and consistent red flag technology, will be useful for early detection of neoplasm in clinical applications.

INDEX TERMS Red flag technique, saliency-aided visual enhancement (SAVE), virtual chromoendoscopy, superficial neoplasm.

I. INTRODUCTION

According to the latest report of World Health Organization, luminal gastrointestinal (esophageal, stomach, and colorectal) cancer is a leading cause of death worldwide, accounting for 1.82 million deaths in 2012 [1]. Early detection of cancer at a curable stage is of critical importance for improving the prognosis and reducing the mortality. Five-year survival rate can significantly be raised from 3.1% to 37.1% for esophageal cancer, from 3.4% to 62.5% for gastric cancer and 11.3% to 90.8% for colorectal cancer, if detected at an early stage (localized) compared to an advanced stage (distant metastases) [2].

Superficial neoplastic lesions are the precursor lesions to gastrointestinal cancer, with varied potential for malignant transformation depending on their type, morphology, anatomic site, and depth of invasion. According to Paris classification, neoplastic lesions with superficial appearance (lesions with assessed depth of invasion limited to mucosa and submucosa) are classified as type-0, which are further divided into polypoid and non-polypoid subtypes. Non-polypoid lesions are now recognized as significant precursors to gastrointestinal cancer, with a higher risk of progression to invasive malignancy, regardless of size [3], [4]. On the contrary to polypoid lesions, where size and stalk expansion are the major indicators for malignancy assessment, macroscopic morphology plays the deciding role for non-polypoid lesions. For example, the depressed subtype with diameter even less than 1 cm has a high risk of submucosal invasion. These factors have stimulated greater interest among researchers and clinicians for improved detection and assessment of non-polypoid lesions.

The detection of non-polypoid lesions using conventional imaging modalities is a challenging task and is associated with unacceptably high miss rate, ranging from 35% to
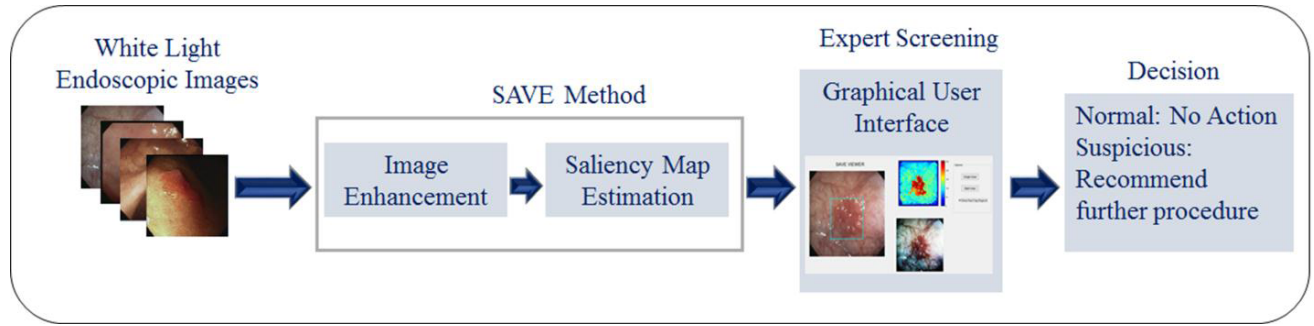
FIGURE 1. Overview of proposed SAVE method.

87% for colorectal cancer [5] and 16% to 23% for gastric cancer [6]. The expertise level of endoscopists plays an important role in the detection of non-polypoid lesions, often characterized by subtle mucosal change. Several image-enhanced endoscopy (IEE) techniques have exhibited promises to facilitate improved visualization and diagnostic yield of subtle lesions. Initial studies suggested that, chromoendoscopy (i.e., spraying of a dye on suspected mucosa) after inspection with white light imaging may be helpful for identification of non-polypoid lesions, especially in stomach and esophagus [3]. However, the labor-intensive and time-consuming nature of the procedure, the need for dye spraying and suction, and the conflicting published data regarding the role of chromoendoscopy [7], [8], have given impetus for extensive investigation of the potential of virtual chromoendoscope techniques. The efficacy of the commercially available virtual chromoendoscope techniques, including narrow band imaging, flexible spectral imaging color enhancement (FICE) and i-scan for non-polypoid lesion detection are not still established and require further clinical studies [6], [9], [10]. Additionally, new imaging technologies are invariably associated with significant learning curve, irrespective of expertise level [11]–[13].

A state-of-the-art method was proposed to automatically highlight the salient regions in endoscopic images, obviating human subjectivity due to level of expertise and awareness [14]. The method exhibited promises for detection and localization of a wide variety of lesions. Motivated by the novel concept of combining image enhancement technique with saliency detection algorithm, in this article, a new screening tool, SAVE (Saliency-aided Visual Enhancement) has been proposed and evaluated for the efficacy of superficial neoplastic lesion detection.

II. SAVE (SALIENCY-AIDED VISUAL ENHANCEMENT) METHOD

SAVE is a two-stage "red-flag" endoscopic imaging technique. The first stage, involving the application of image enhancement on the white light endoscopic (WLE) images, is essentially a virtual chromoendoscopy system. The second stage employs a saliency detector on the color enhanced image and highlights the suspicious regions.

Therefore, SAVE will provide both qualitative enhancement and quantitative suspicion index to draw attention to a region containing abnormality. An overview of the proposed method is depicted in Fig. 1.

A. FIRST STAGE: IMAGE ENHANCEMENT

Image enhancement is a post-processing algorithm, applied on the WLE images. Image enhancement algorithm consists of two consecutive steps: contrast enhancement and color enhancement. In the following section, a brief overview of the steps of image enhancement stage will be given.

1) CONTRAST ENHANCEMENT

The aim of contrast enhancement is to improve the visual appearance of an image by sharpening edge or texture components of the image. In this paper, an Unsharp Masking approach has been adopted for contrast enhancement. Unsharp Masking exploits "simultaneous contrast", a property of human visual system, where the difference in the perceived brightness of adjacent regions depends on the sharpness of the transition [15]. In this method, a fraction of the highpass filtered version of the image is added to the original image to enhance sharpness along the edges and therefore to enhance the contrast of the image. Unsharp Masking is a popularly used image processing technique [15]–[17] and also has been extensively used in medical imaging [18], [19].

Mathematically, linear Unsharp Masking can be represented as:

$$y(m, n) = x(m, n) + \lambda z(n, m) \tag{1}$$

Here, $z(m, n)$ is the high-pass filtered version of the original signal $x(m, n)$ and λ is a user-defined sharpening factor that controls the level of contrast enhancement. λ is adaptively selected with relation to the input image using the following equation:

$$\lambda = \alpha \frac{\sum x(m, n)}{N} \tag{2}$$

Here, N is the total number of pixels in the image and α is the scaling factor. As the value of α increases, sharpness of the image increases and after a certain limit, image quality starts to degrade.
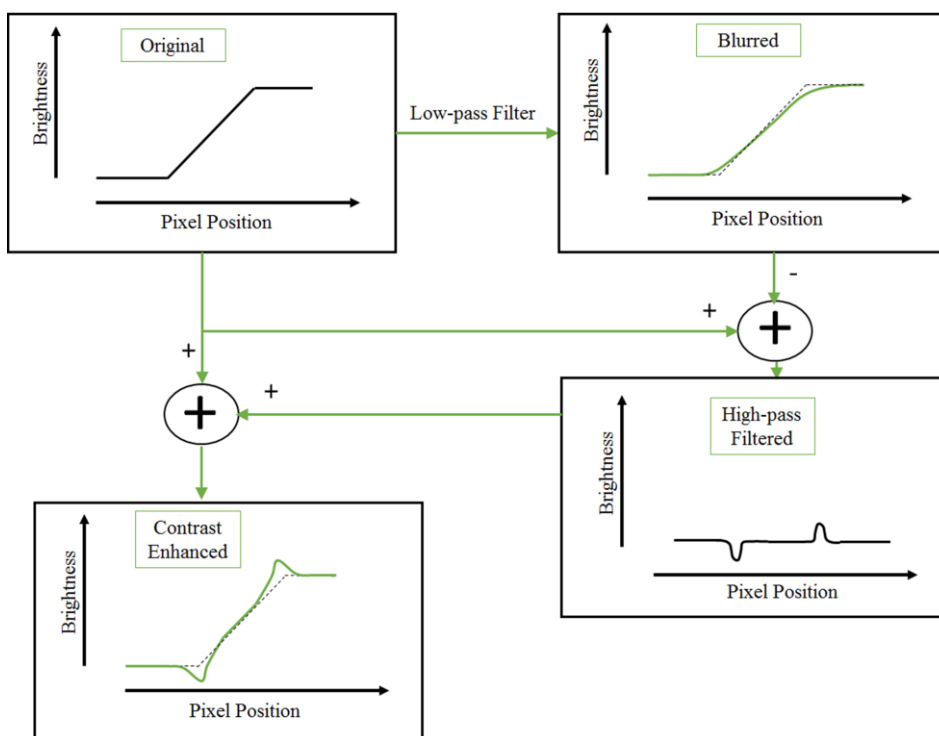
FIGURE 2. Visual depiction of contrast enhancement method.

The high-pass filtered signal is achieved by subtracting a blurred or smoothed version (obtained by low-pass filtering) of the image from the original image.

$$z(n, m) = x(m, n) - x_{blurred}(m, n) \qquad (3)$$

A visual depiction of the principle of contrast enhancement is given in Fig. 2.

2) COLOR ENHANCEMENT
The aim of color enhancement is to enhance the vascular and surface structure of the mucosa in the WLE images. Conventional white light endoscopy uses full visible wavelength to produce an image. However, light with specific wavelength is useful to visualize the pattern of certain layer into the mucosa. The wavelength of the light determines the penetration depth into the mucosa. Short wavelength light, ranging from 400-430 nm (corresponding to blue light), has a shallow penetration depth. Therefore, blue light is best-suited to enhance the superficial mucosa structure and to detect the minute mucosal change. Additionally, blue light, as it corresponds to the absorption peak of hemoglobin, enables detailed inspection of microvasculature (intraepithelial papillary capillary loops) on the mucosal surface. Green light, with wavelengths of 525- 555 nm, has a deeper penetration depth, corresponds to the second peak of hemoglobin absorption spectra, and is useful for the visualization of thick blood vessels located at the intermediate layer of mucosa (muscularis mucosa). Therefore, blue and green wavelength lights have distinct advantage for the detection of subtle mucosal
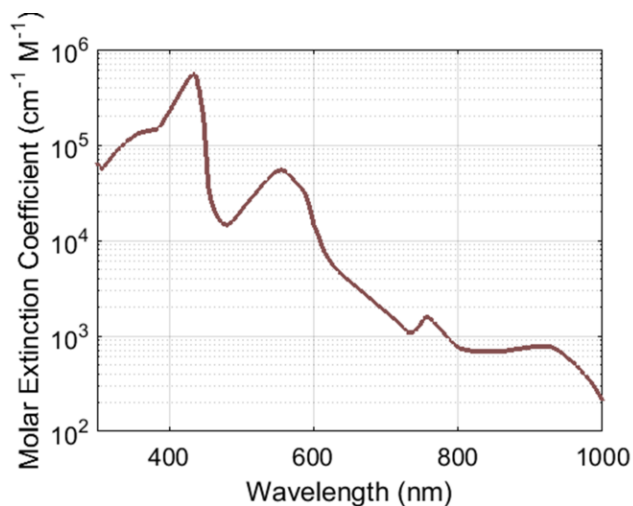

FIGURE 3. Absorption spectra of hemoglobin.

lesions and inspection of capillary vessels in different layers of mucosa [20]–[22]. The absorption spectra of Hemoglobin has been depicted in Fig. 3, which shows two absorption peaks corresponding to wavelengths of blue and green light.

To capture the image features visible in green and blue light, the white light endoscopic images are processed accordingly in the color enhancement step. The red component of the endoscopic image is suppressed by a histogram modification technique, where red intensity values are transformed following a modified transform-based γ is the γ correction
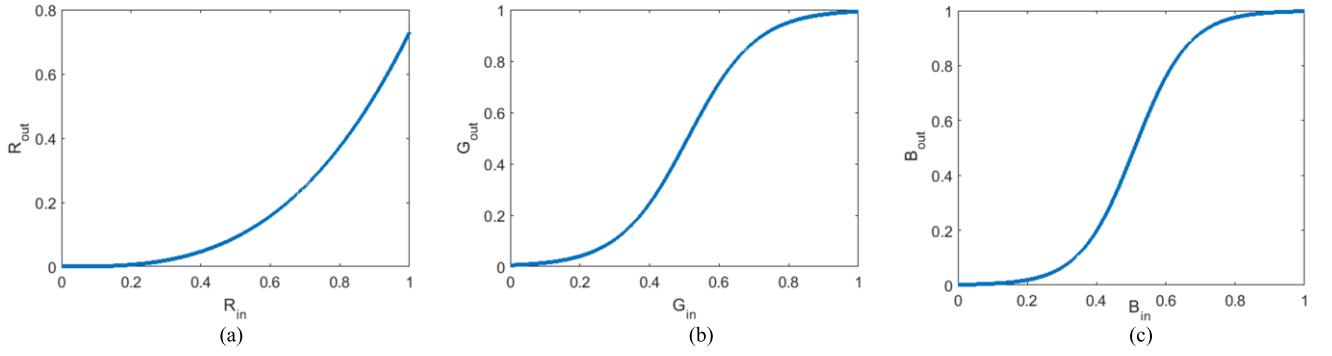
FIGURE 4. Color enhancement curves for (a) Red (b) Green and (c) Blue components.
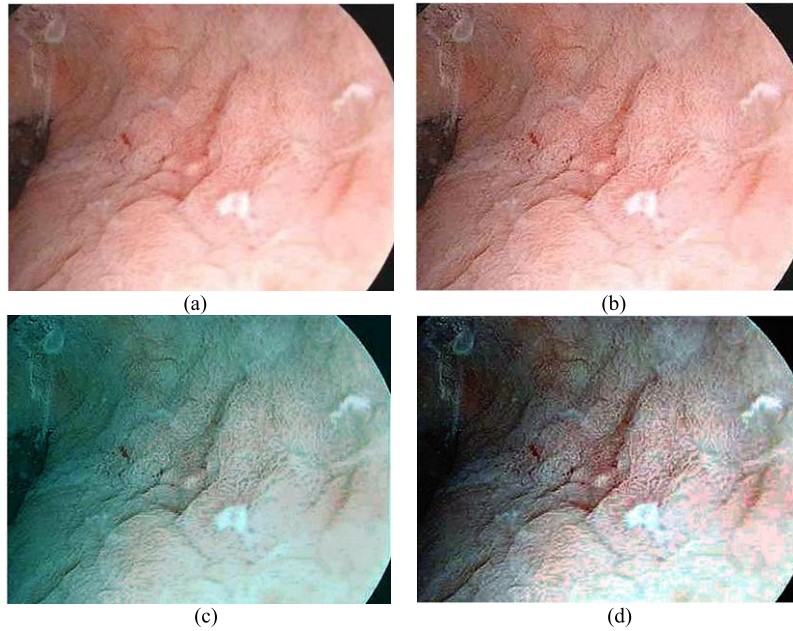

FIGURE 5. Steps of image enhancement: (a) Original WLE image, (b) Image after contrast enhancement, (c) Image after color enhancement, (d) Final image.

factor,

$$T(l) = (l_{max} - s)(l/l_{max})^\gamma \tag{4}$$

where l_{max} is the maximum intensity of the input, γ is the gamma correction factor, and s is the amount of suppression. The intensity l of each pixel in the input image is transformed according to $T(l)$.

The green and blue components of the endoscopic images are contrast enhanced by utilizing a sigmoidal remapping curve. To enhance the perceived image contrast in the limited dynamic range, both the regions with high intensity and very low intensity have been compressed, whereas the intermediate intensity regions have been stretched [23]. The sigmoidal remapping function is given by:

$$T(l) = l_{max} \cdot \frac{1}{1 + e^{-a(l-c)}} \tag{5}$$

where a and c are the parameters, which control the shape of the function. Based on eq. (3) and eq. (4), separate color

enhancement curves are formed for red, green and blue color channel (Fig. 4). The coefficient values for the equations are empirically selected for optimum performance. Finally, histogram equalization is performed on each color channel to form the final image. Fig. 5 shows resultant images after performing each step of image enhancement.

B. SECOND STAGE: SALIENCY MAP ESTIMATION
The second stage involves the computation of saliency map from the enhanced image obtained in the first stage. Motivated by the attention mechanism of human visual system, the saliency detection algorithm is aimed at capturing the most informative image region without any prior learning. Unlike image enhancement, which qualitatively improves visualization of clinically significant features, saliency map is aimed at providing a quantitative score of image regions based on their distinctness compared to the neighborhood regions. A region with high saliency score signals a red-flag
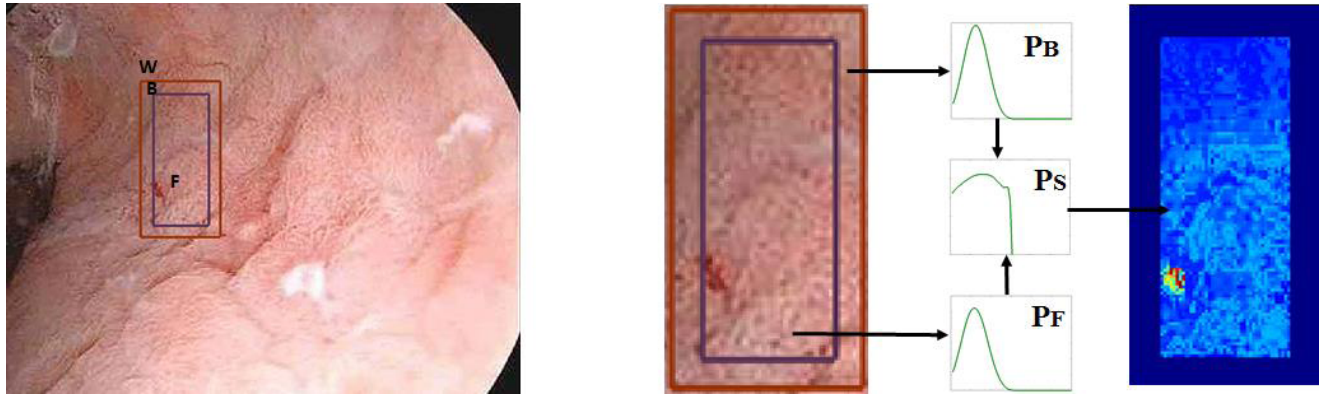
FIGURE 6. Outline for Saliency map estimation. *W* is a sliding window, divided into outer boundary *B* and inner box *F*. P_B : conditional feature distribution computed from histogram of features in *B*. P_F : conditional feature distribution computed from histogram of features in *F*. P_S : Probability distribution of estimated saliency map. Saliency map obtained for one window position has been shown.

and indicates that careful examination of the corresponding region is required.

To estimate the saliency map from the enhanced endoscopic image, the method proposed in [24] has been adopted. The method is based on a sliding window approach, where the saliency of a point in the window is computed using Bayes theorem by determining intensity distribution inside the window compared to the intensity distribution of the surrounding area.

Let *W* be a rectangular window, which is divided into an inner box *F* and outer boundary *B*. Let, *x* be a point inside *W*. The feature $C(x)$ considered for distribution computation at pixel *x* are the three color components in CIE Luv color space. On the basis of the initial assumption that the pixels inside *F* are salient, and outside *F* are non-salient, the conditional feature distribution $p(C(x)|H_1)$ and $p(C(x)|H_0)$ are computed from the normalized histogram of the feature values in *F* and *B*. Here, H_0 is the hypothesis that point *x* is not salient, and H_1 is the hypothesis that *x* is salient, associated with the priori probabilities $P(H_0)$ and $P(H_1)$. Writing the conditional feature distribution $p(C(x)|H_1)$ and $p(C(x)|H_0)$ as P_F and P_B respectively, Bayes' theorem gives the probability P_s of the pixel *x* being salient as:

$$P_S = P(H_1 | C(x)) = \frac{P_F P(H_1)}{P_B P(H_0) + P_F P(H_1)} \qquad (6)$$

Using equation (6), we can compute the probability that a pixel is salient, for each pixels in *F* overwriting the initial assumption of H_1. Finally, the window *W* slides over the image with a certain step size, s_w. Let, $W(i)$ be the window centered at pixel position *i* and $S_i(x)$ is the saliency for a point *x* for this window position. For the overlapping windows sliding over the image and also for three different color channels, multiple saliency measures will be obtained for each point. The final saliency of a point is computed by taking the maximum:

$$S(x) = \max_{j}\{S_j(x) | x \in W(j)\} \qquad (7)$$

Since the neoplastic lesions may appear in several scales, the algorithm was run with four different window sizes. The saliency value of the pixel is taken as a maximum over all scales. The algorithm intends to find the pixels in the inner box *F*, which are well-described by the intensity distribution of *F*, compared to the intensity distribution of the border *B*. A key assumption for the algorithm is that the distribution of a salient object will be significantly different from the background intensity distribution. An overview of the saliency map estimation algorithm is given in Fig. 6.

C. SAVE: GUIDELINE FOR USE IN CLINICAL PRACTICE

For each endoscopic image, SAVE generates two images: one is the qualitatively enhanced image, and another one is the estimated saliency map. A user-friendly and practically feasible user-interface has been proposed in this paper, which will enable the physicians to choose between single view and multiple view (Fig. 7). Single view will allow to screen only the original images, while Multiview will display SAVE generated images along with the original image. Turning on the push button ''Show Red-Flag Regions'' will draw boundary boxes enclosing the suspicious regions according to the score obtained from saliency map. According to physicians, the Multiview mode along with the boundary box around the suspicious regions aids to make better decision. From the visual inspection, physicians can retain the suspicious regions, which may require further investigation, i.e., chromoendoscopy, magnification, or biopsy and discard the innocuous ones.

III. METHODOLOGY EVALUATION
A. IMAGES

In the experiment, a total of 40 images containing early neoplastic lesions are included, which are part of the material used in previous studies [25]. The lesions are classified into type I, IIa, IIb, IIc and IIc+IIa based on their macroscopic appearances according to Paris Classification [3]. A description of the lesions is given in Table 3. These lesions are
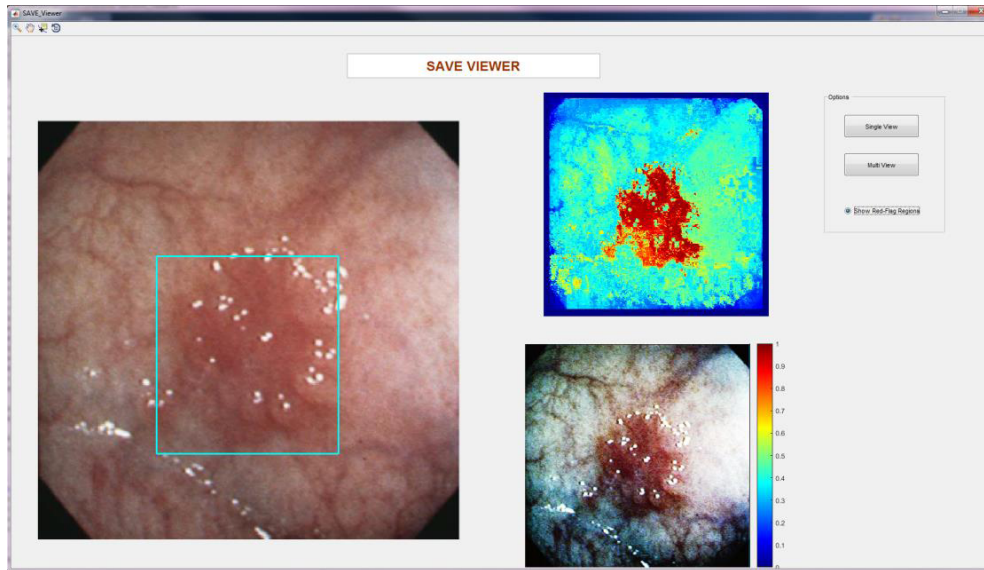
FIGURE 7. Graphical user interface for SAVE.

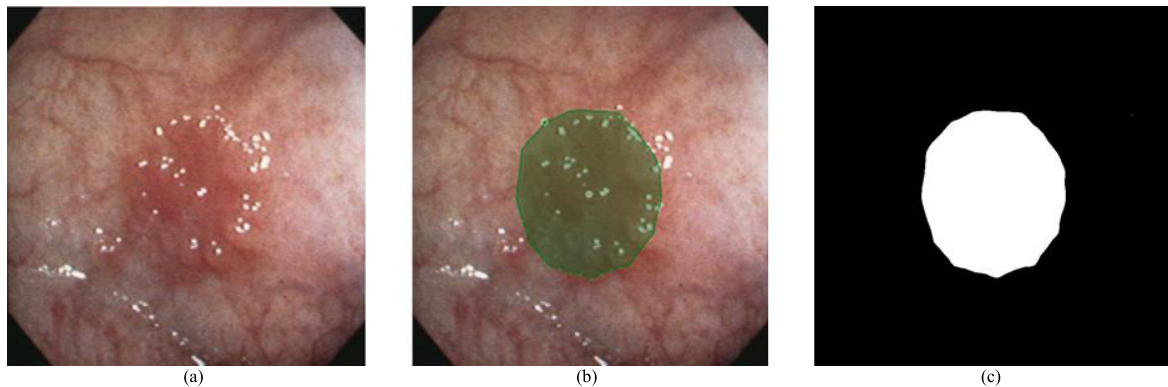
(a)   (b)   (c)

FIGURE 8. Criterion-standard image annotation and mask formation using Ratsnake software. (a) Original image containing neoplastic lesion of type IIc+IIa in ascending colon; (b) Graphical annotation using Ratsnake software; (c) Resulting mask.

accompanied with the histological specimens (biopsy and resection). Detailed endoscopic and pathological description highlighting both the Western and Japanese point of view is available for these images, which forms the ground truth for the experiment. According to physician feedback and by using histopathology determination as the criterion standard, the lesions in the images were annotated using Ratsnake [26], a publicly available software for image annotation and then exported as masks to conduct methodology evaluation. An example for lesion annotation is shown in Figure 8.

Additionally, 55 normal images were included into the dataset to analyze the discriminating ability of SAVE between clinically significant and non-significant images. These images are available online [27].

B. STATISTICAL METHODS

Statistical analysis was performed using MATLAB 2015a (The MathWorks Inc., Natick, Massachusetts, USA). The data were assessed with the nonparametric Mann-Whitney U test and the Kruskal-Wallis test, where a P-value<0.05 was considered as statistically significant.

TABLE 1. Description of experimental dataset.

Total no. of Lesions	40
Location, no.	
Esophagus	15
Stomach	20
Colon	4
Rectum	1
Macroscopic type, no.	
0-IIa	10
0-IIb	6
0-IIc	14
Mixed (0-IIa+0-IIc)	10

To evaluate the efficacy of SAVE, we perform both CAD-based and expert-opinion based evaluation. The CAD-based evaluation measures the extent to which

TABLE 2. Parameter base values and impact of parameter variation (±10%).

Parameter	Description	Value	*MAD*	δ (*overlap_index*)
α	Sharpening factor in Unsharp Masking eqn (2)	5	0.90	0.06
γ	Gamma correction parameter eqn (4)	3	1.14	0.08
s	Intensity Suppression parameter eqn (4)	0.25	1.08	0.03
a	Sigmoidal remapping function parameter eqn (5)	0.04 (G) 0.05 (B)	10.07 (G) 5.37 (B)	6.25 (G) 4.02 (B)
c	Sigmoidal remapping function parameter eqn (5)	$l_{max}/2$	4.29 (G) 2.32 (B)	4.89 (G) 1.25 (B)
w_W	Window width in saliency map estimation	$[0.25, 0.3, 0.5, 0.7]$ $\cdot \max\{w, h\}$		
h_W	Window height in saliency map estimation	$[0.1, 0.3, 0.4, 0.5]$ $\cdot \max\{w, h\}$	3.93	4.83
B_t	Thickness of the outer box	$0.1 \cdot \max\{w, h\}$		
s_w	Sampling step	$[0.01, 0.015, 0.03, 0.04] \cdot$ $\max\{w, h\}$		

* w and h are respectively the width and height of the input image.
* G= Green Channel, B= Blue Channel

TABLE 3. Expert opinion on SAVE (presented as percentage of total cases).

	Strongly Agree	Agree	Neutral	Disagree
SAVE will be useful for type 0 neoplastic lesion detection	10%	70%	20%	0%

SAVE recognizes clinically significant regions. We define two metrics for evaluating the performance: *Overlap Index* and *Mean Saliency Score(MSS)*.

Overlap Index

$$= \frac{\text{Area Overlap between ROI in Original image and SAVE Generated Binary Map}}{\text{Area of ROI in Original image}}$$

Overlap Index can have value from 0 to 1, where 0 corresponds to no overlap and 1 corresponds to perfect overlap. The binary map for *Overlap Index* calculation was computed by thresholding the SAVE generated Saliency Map. *Overlap Index* measures the extent to which the highlighted region in SAVE generated saliency map coincides with the lesion area in the original image and thus is a measure of localization capability of SAVE.

On the other hand, *Mean Saliency Score* is computed by thresholding the saliency map and averaging the saliency score of connected regions in the resulting binary map. Though a number of irrelevant regions are highlighted in the saliency map along with the clinical significant ones, the later are associated with a higher *MSS*. The classification between lesion and non-lesion images will be performed based on *MSS* and the classification performance will be assessed by receiver-operating characteristic (ROC) analysis.
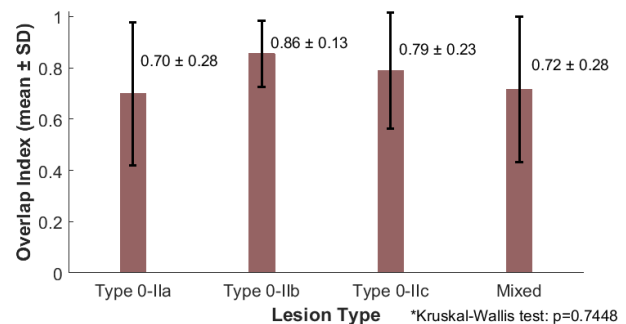

FIGURE 9. Overlap index for superficial non-polypoid neoplastic lesions with different macroscopic appearance.

C. THE CHOICE OF PARAMETERS AND ROBUSTNESS

The proposed SAVE method involves certain number of parameters. A complete list of the parameters and their values used in the experiments is given in Table 2. The parameter values were tuned based on a subset of the database constituting 10 images: five containing neoplastic lesions and five normal images. Instead of fine-tuning of the parameters to ensure the best performance, we rely on selecting an intermediate value among a range of values providing reasonable performance. The objective was to ensure that the performance of the proposed method is not too much sensitive to slight variation in parameter values.

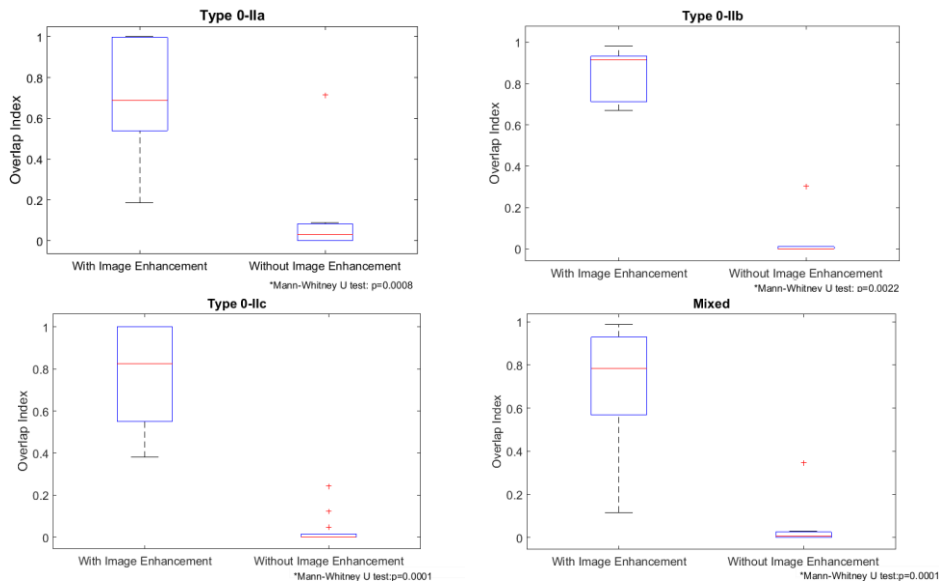To evaluate the impact of the parameters on the performance of the algorithm, we perturb one parameter at a time

FIGURE 10. Box and whisker representation of *Overlap Index* obtained from SAVE method with and without image enhancement.

and keep the other parameters fixed at their base values. In case of parameters involved in saliency map estimation, all the four parameters were changed together to maintain the proportionality. Then, we measure the mean absolute difference (*MAD*) between the saliency map obtained using the base value and the perturbed value. Also, we compute the percentage change in overlap index ($\delta(overlap\_index)$) resulted from the variation in the parameter base value. In this experiment, the parameter values were changed by $\pm 10\%$, a substantial perturbation, which ensures a comprehensive understanding of the impact of the parameter values on the performance of the proposed algorithm.

D. RESULTS

SAVE was able to highlight the neoplastic region areas in all of the 40 images. A comparative analysis was performed to compute the overlap between SAVE generated binary image and original image for lesions with different morphological type. On an average, SAVE resulted in overlapping of 70% for type 0-IIa (elevated) lesions, 86% for 0-IIb (flat) lesions, 79% for 0-IIc (depressed) lesions and 72% for mixed lesions (Fig. 9). Performing the Kruskal-Wallis test, we found that the *Overlap Index* values (p=0.7448) were not significantly different among different lesion types.

SAVE is essentially a virtual chromoendoscope technique, further associated with a saliency detection tool. To emphasize on the importance of the virtual chromoendoscopy step, a comparison between *Overlap Index* values obtained from two methods, SAVE with and without virtual chromoendoscopy step, was performed. From the box-whisker plot presented in Fig. 10, it can be seen that overlap index values obtained without image enhancement are significantly lower than those obtained with image enhancement for type 0-IIa (p=0.0008), type 0-IIb (p=0.0022), type 0-IIc (p=0.0001)
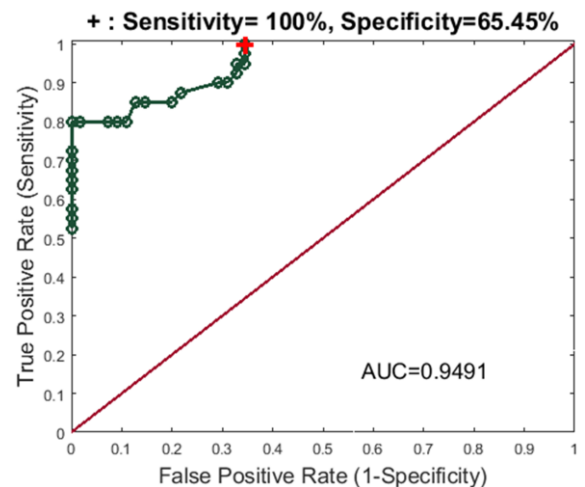

FIGURE 11. ROC curve for frame-wise classification using *MSS* criterion. Red + mark the point selected for classification.

and mixed (p=0.0001) type of neoplastic lesions.

The ability of SAVE to discriminate between images containing lesions and normal images was assessed by receiver-operating characteristic (ROC) analysis and quantified by the area under ROC curve. Different cut-off values for *Mean Saliency Score*(*MSS*) correspond to different points of ROC curve in Fig. 11. As SAVE will act as a screening tool and will assist the physicians to point to the suspicious regions, achieving a high (preferably perfect) sensitivity was the major concern. Therefore, a cut-off value of *MSS* was selected which resulted in perfect sensitivity (100%) and moderate specificity (65.45%). The AUC value 0.9491 indicated the high discriminating power of SAVE.

To evaluate the impact of the parameters on the performance of SAVE, a robustness study was performed.

The results of the robustness experiment have been given in Table 2. We observe that all the parameters involved in SAVE are very robust, with an exception to sigmoidal remapping function parameter, a for green channel. For a 10% relative perturbation of the parameters, both performance metric *MAD* and δ *(overlap_index)* are around 5% or below, except for sigmoidal remapping function parameter, a for green channel. Therefore, the proposed system is quite robust against the variation in the parameters.

For the expert evaluation, the images were evaluated by an experienced gastroenterologist who was blinded to the clinical background and histological outcome. According to the expert opinion, SAVE would be useful for decision making in majority of cases (70%) (Table 3). There was significant improvement in sensitivity (11.11%) in detecting neoplastic lesion using SAVE compared to white-light endoscopic observation alone. However, the specificity remained unchanged.

IV. DISCUSSION AND CONCLUSION

Several studies show that, targeted biopsy, performed with the help of red flag techniques significantly increases diagnostic yield of superficial neoplasm compared to the standardized surveillance practice of white light endoscopy and random biopsy [28]–[30]. To be ideal for the clinical use, a red-flag technique should be cost-effective, easy-to-use, highly sensitive, moderately specific and consistent resulting in minimal inter-observer variability [31]. The current endoscopic imaging techniques (including chromoendoscopy and virtual chromoendoscopy) are invariably associated with learning effect to varying extent, as the identification of suspicious regions depends on the knowledge and experience of the physician. Therefore, inter-observer variability is inherently present in these methods. The objective of our proposed method is to introduce automation to highlight the potentially suspicious regions in the image. Similar to the currently existing VCE systems, the proposed system performs image enhancement on the WLE images to visually enhance the image features. The major difference of the proposed system compared to the existing VCE systems is that it has an additional processing stage to quantify the significance or suspicion index of image regions. The quantification of significance, calculated based on human visual attention mechanism, serves two purposes: (1) the inter-observer variability is eliminated; the automatic detection of red-flag regions aids the physicians for primary identification independently of prior experience; (2) missing rate of subtle lesions is reduced; very high sensitivity for a dataset containing difficult-to-identify lesions suggests that the method ensures detection of minute lesions.

In Fig. 12, four example images have been demonstrated containing neoplastic lesions with varying visibility [25]. Each image is associated with corresponding chromoendoscopic image (obtained by spraying dye at the same site) and SAVE generated saliency map. The suspected region found from the saliency map is annotated by a boundary box in the original image. In all the cases, we can see that the mucosal irregularities captured in the chromoendoscopic images have also been highlighted in the respective saliency map. In case A, a lesion with macroscopic appearance of type 0-IIc was found at the greater curvature of the antrum. The biopsy and mucosectomy specimen reveal a well-differentiated adenocarcinoma with sub-mucosal invasion. However, according to the expert opinion (specifically, western endoscopists), this lesion will not be suspected and any further procedure, e.g., dye spraying and biopsy will not be undertaken. The SAVE generated saliency map with significantly high saliency score at the lesion area could suggest the physician to examine the lesion closely and improve the decision. Case B demonstrates a type 0-IIc neoplastic lesion with slight depression and reddening. The irregular shape and size were delineated after iodine staining, which suggests a submucosal invasion. Case B is one of the examples where the lesion was erroneously labelled as non-neoplastic from WLE image and then labelled as neoplastic with the aid of SAVE generated images. Case C presents a type 0-IIc+IIa lesion in the descending colon, with visually evident aggressive nature. The lesion was diagnosed as a well-differentiated adenocarcinoma with submucosal invasion from the microscopic findings. In this case, SAVE successfully identifies and highlights the affected region. Case D shows a type 0-IIb neoplastic lesion in the esophagus. The lesion was only visible after iodine staining. SAVE generated saliency map perfectly highlights the mucosal irregularity and therefore improves the chance of detection. These examples show that SAVE method can accentuate lesion areas with varying visibility with a comparable performance to the chromoendoscopy.

The experimental results show the efficacy of the proposed method. The *Overlap Index* was calculated to measure the extent SAVE can detect the lesion areas. Based on the assumption that a minimum of 50% overlap (to the ground truth lesion) is required to identify a possible suspected lesion, the proposed method can successfully detect all types of lesions with an average *Overlap Index* > 0.7. We also experimented to evaluate the contribution of image enhancement stage of SAVE method for the detection of lesions. A comparative study showed that the performance of the proposed system without image enhancement is significantly inferior in terms of *Overlap Index* compared to that with image enhancement. As a red-flag technique, the proposed method required to have a very high sensitivity and moderate specificity. From the receiver-operating characteristic, it can be seen that SAVE can attain very high sensitivity (100% for the used dataset) and moderate specificity. Additionally, the robustness study demonstrated that the proposed system is quite robust against the variation in the parameters, except for sigmoidal remapping function parameter for green channel. However, the parameter values are system dependent, not patient dependent. Therefore, the parameters can be pre-tuned for a specific system, which makes it implementable in the practical application.

There are several limitations to this study. As the proposed method is a screening tool, rather than an automatic
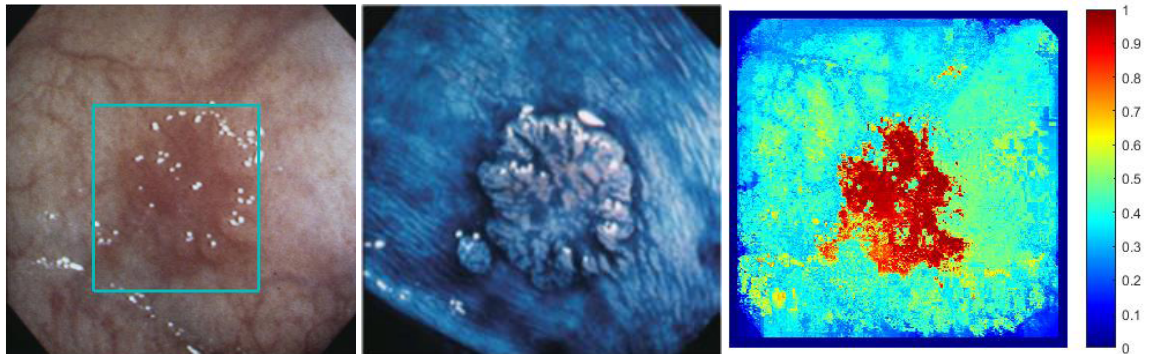
Case A
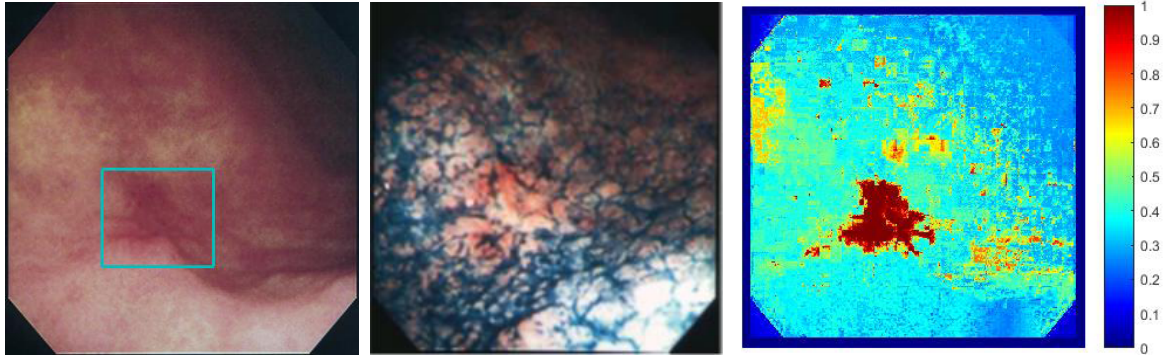
Case B
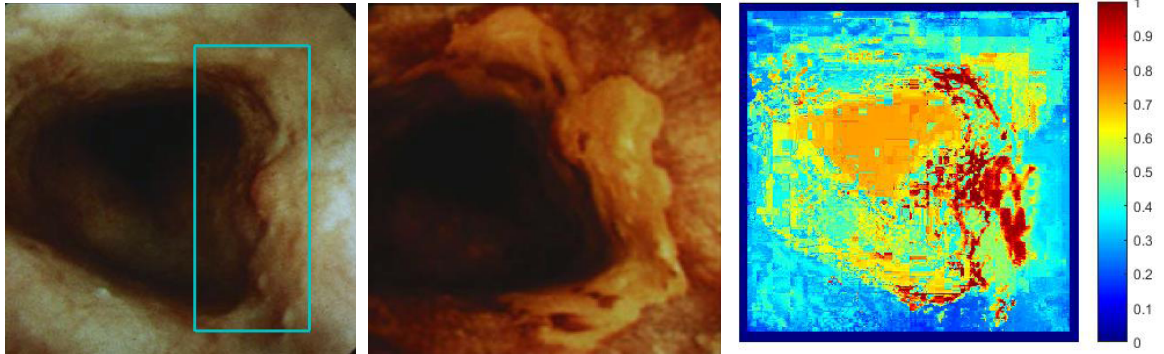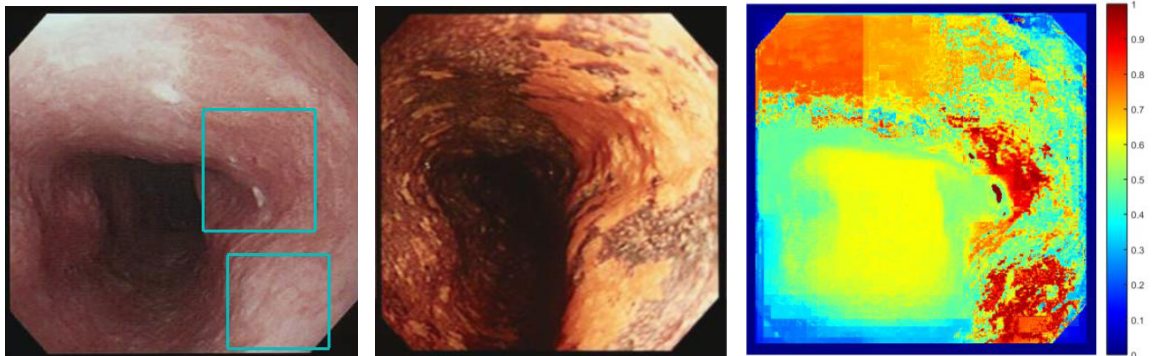
Case C

Case D

FIGURE 12. Example of images containing superficial neoplastic lesions [25]. Left Column: Original image with the boundary box denoting the suspicious region. The boundary box is formed using the information from the respective saliency map. Middle column: Chromoendoscopic images (obtained after spraying dye at the same site). Right column: SAVE generated saliency map.

detection system, the sensitivity and specificity measures should be based on the decision made by the physicians. In this study, only one expert was involved who suggested that SAVE method can significantly improve the visualiza-

tion and decision quality. In the future work, an extensive study with a large dataset and involving a group of experts will be performed to establish the primary promise of the proposed method. However, based on the comparison to the

chormoendoscopic images obtained by spraying dye, the SAVE method is expected to give diagnostic yield comparable to chemical chromendosocpy and thus offers a simple and effective alternative to chromendosocpy.

ACKNOWLEDGMENT

REFERENCES

[1] B. W. Stewart and C. P. Wild, "World cancer report 2014," Int. Agency Res. Cancer, Lyon, France, Tech. Rep, 2014.

[2] M. J. Horner *et al.*, "SEER cancer statistics review, 1975–2006," Nat. Cancer Inst., Bethesda, MD, USA, Tech. Rep., 2009, pp. 545–576.

[3] H. Inoue *et al.*, "The Paris endoscopic classification of superficial neoplastic lesions: Esophagus, stomach, and colon: November 30 to December 1, 2002," *Gastrointestinal Endoscopy*, vol. 58, no. 6, pp. S3–S43, 2003.

[4] A. Axon *et al.*, "Update on the Paris classification of superficial neoplastic lesions in the digestive tract," *Endoscopy*, vol. 37, no. 6, pp. 570–578, 2005.

[5] B. Levin *et al.*, "Screening and surveillance for the early detection of colorectal cancer and adenomatous polyps, 2008: A joint guideline from the American Cancer Society, the US Multi-Society Task Force on Colorectal Cancer, and the American College of Radiology," *CA, A Cancer J. Clin.*, vol. 58, no. 3, pp. 130–160, 2008.

[6] M. Song and T. L. Ang, "Early detection of early gastric cancer using image-enhanced endoscopy: Current trends," *Gastrointestinal Interv.*, vol. 3, no. 1, pp. 1–7, 2014.

[7] S. Ngamruengphong, V. K. Sharma, and A. Das, "Diagnostic yield of methylene blue chromoendoscopy for detecting specialized intestinal metaplasia and dysplasia in Barrett's esophagus: A meta-analysis," *Gastrointestinal Endoscopy*, vol. 69, no. 6, pp. 1021–1028, 2009.

[8] Y. Nagami *et al.*, "Usefulness of non-magnifying narrow-band imaging in screening of early esophageal squamous cell carcinoma: A prospective comparative study using propensity score matching," *Amer. J. Gastroenterol.*, vol. 109, no. 6, pp. 845–854, 2014.

[9] S. J. Chung *et al.*, "Efficacy of computed virtual chromoendoscopy on colorectal cancer screening: A prospective, randomized, back-to-back trial of Fuji Intelligent Color Enhancement versus conventional colonoscopy to compare adenoma miss rates," *Gastrointestinal Endoscopy*, vol. 72, no. 1, pp. 136–142, 2010.

[10] J. W. Rey, R. Kiesslich, and A. Hoffman, "New aspects of modern endoscopy," *World J. Gastrointestinal Endoscopy*, vol. 6, no. 8, p. 334, 2014.

[11] P. J. Basford, G. R. Longcroft-Wheaton, and P. Bhandari, "The learning curve for *in-vivo* characterisation of small colonic polyps: Number needed to train (NNT) is 200 polyps," *Gastrointestinal Endoscopy*, vol. 5, no. 77, p. AB528, 2013.

[12] G. Galloro, S. Ruggiero, T. Russo, and B. Saunders, "Recent advances to improve the endoscopic detection and differentiation of early colorectal neoplasia," *Colorectal Disease, Off. J. Assoc. Coloproctol. Great Brit. Ireland*, vol. 17, pp. 25–30, Jan. 2015.

[13] A. Adler *et al.*, "A prospective randomised study on narrow-band imaging versus conventional colonoscopy for adenoma detection: Does narrow-band imaging induce a learning effect?" *Gut*, vol. 57, no. 1, pp. 59–64, 2008.

[14] F. Deeba, S. K. Mohammed, F. M. Bui, and K. A. Wahid, "Unsupervised abnormality detection using saliency and retinex based color enhancement," in *Proc. 38th Annu. Int. Conf. IEEE Eng. Med. Biol. Soc.*, Aug. 2016, pp. 3871–3874.

[15] G. Ramponi, N. Strobel, S. K. Mitra, and T.-H. Yu, "Nonlinear unsharp masking methods for image contrast enhancement," *J. Electron. Imag.*, vol. 5, no. 3, pp. 353–366, 1996.

[16] T. Luft, C. Colditz, and O. Deussen, "Image enhancement by unsharp masking the depth buffer," *ACM Trans. Graph.*, vol. 25, no. 3, pp. 1206–1213, 2006.

[17] G. Deng, "A generalized unsharp masking algorithm," *IEEE Trans. Image Process.*, vol. 20, no. 5, pp. 1249–1261, May 2011.

[18] T. H. Khan, S. K. Mohammed, M. S. Imtiaz, and K. A. Wahid, "Color reproduction and processing algorithm based on real-time mapping for endoscopic images," *SpringerPlus*, vol. 5, no. 1, p. 17, 2016.

[19] K. Panetta, Y. Zhou, S. Agaian, and H. Jia, "Nonlinear unsharp masking for mammogram enhancement," *IEEE Trans. Inf. Technol. Biomed.*, vol. 15, no. 6, pp. 918–928, Nov. 2011.

[20] J. Y. Jang, "The usefulness of magnifying endoscopy and narrow-band imaging in measuring the depth of invasion before endoscopic submucosal dissection," *Clin. Endosc.*, vol. 45, no. 4, pp. 379–385, 2012.

[21] N. Yoshida, N. Yagi, Y. Inada, M. Kugai, A. Yanagisawa, and Y. Naito, "Therapeutic and diagnostic approaches in colonoscopy," in *Endoscopy of GI Tract*. Rijeka, Croatia: InTech, 2013, pp. 233–263.

[22] Y. Sano, M. Muto, H. Tajiri, A. Ohtsu, and S. Yoshida, "Optical/digital chromoendoscopy during colonoscopy using narrow-band imaging system," *Digestive Endoscopy*, vol. 17, no. s1, pp. S43–S48, 2005.

[23] G. J. Braun and M. D. Fairchild, "Image lightness rescaling using sigmoidal contrast enhancement functions," *J. Electron. Imag.*, vol. 8, no. 4, pp. 380–393, 1999.

[24] E. Rahtu and J. Heikkilä, "A simple and efficient saliency detector for background subtraction," in *Proc. IEEE 12th Int. Conf. Comput. Vis. Workshops (ICCV Workshops)*, Sep. 2009, pp. 1137–1144.

[25] R. Fujita, J. R. Jass, M. Kaminishi, and R. J. Schlemper, *Early Cancer of the Gastrointestinal Tract*. Tokyo, Japan: Springer-Verlag, 2006.

[26] D. K. Iakovidis, T. Goudas, C. Smailis, and I. Maglogiannis, "Ratsnake: A versatile image annotation tool with application to computer-aided diagnosis," *Sci. World J.*, vol. 2014, Jan. 2014, Art. no. 286856.

[27] A. Koulaouzidis and D. K. Iakovidis. *KID: Koulaouzidis-Iakovidis Database for Capsule Endoscopy*, accessed on Jun. 12, 2016. [Online]. Available: http://is-innovation.eu/kid

[28] B. J. Qumseya *et al.*, "Advanced imaging technologies increase detection of dysplasia and neoplasia in patients with barrett's esophagus: A meta-analysis and systematic review," *Clin. Gastroenterol. Hepatol.*, vol. 11, no. 12, pp. 1562–1570, 2013.

[29] A. Facciorusso, M. Antonino, M. D. Maso, M. Barone, and N. Muscatiello, "Non-polypoid colorectal neoplasms: Classification, therapy and follow-up," *World J. Gastroenterol.*, vol. 21, no. 17, pp. 5149–5157, 2015.

[30] H. Neumann, M. Vieth, C. Langner, M. F. Neurath, and J. Mudter, "Cancer risk in IBD: How to diagnose and how to manage DALM and ALM," *World J. Gastroenterol.*, vol. 17, no. 27, pp. 3184–3191, 2011.

[31] P. Saxena and M. I. Canto, "Red flag imaging techniques in Barrett's Esophagus," *Gastrointestinal Endoscopy Clin. North Amer.*, vol. 23, no. 3, pp. 535–547, 2013.

FARAH DEEBA (S'15) received the B.Sc. degree in electrical and electronic engineering from the Bangladesh University of Engineering and Technology, Dhaka, Bangladesh, in 2013, and the M.Sc. degree in electrical and computer engineering from the University of Saskatchewan, Canada, in 2016. Her research interest includes medical image analysis, computer-aided detection system design, computer vision, and machine learning.

SHAHED K. MOHAMMED (S'15) received the B.S. degree (Hons.) in electrical and electronic engineering from the Bangladesh University of Engineering and Technology, Dhaka, Bangladesh, in 2013, and the M.Sc. degree from the University of Saskatchewan, Canada, in 2017. From 2013 to 2014, he served as a Lecturer with United International University, Dhaka. His research interest includes medical imaging, computer aided detection system, wireless implantable, and wireless capsule endoscopy system.

Mr. Mohammed received the CGSR Scholarship from the University of Saskatchewan and the Dean Scholarship from the Bangladesh University of Engineering and Technology.

FRANCIS MINHTHANG BUI (S'99–M'08) received the B.A. degree (Hons.) in French language and the B.Sc. degree (Hons.) in electrical engineering from the University of Calgary, Calgary, AB, Canada, in 2001, and the M.A.Sc. and Ph.D. degrees in electrical engineering from the University of Toronto, Toronto, ON, Canada, in 2003 and 2009, respectively. He is currently an Assistant Professor of Electrical and Computer Engineering with the University of Saskatchewan, Saskatoon, SK, Canada. His research interests include information processing and optimization, with applications in communications and biomedical engineering.

KHAN A. WAHID received the degree from the Bangladesh University of Engineering and Technology in 2000 and the M.Sc. and Ph.D. degrees from the University of Calgary, Canada, in 2003 and 2007, respectively. He is currently an Associate Professor with the Department of Electrical and Computer Engineering, University of Saskatchewan. In addition to two patents, he has authored or co-authored two book chapters and over 130 peer-reviewed journal and international conference papers in the field of FPGA-based digital system design, video and image processing, embedded systems, biomedical imaging systems, and health informatics. He was a recipient of a Killam Scholarship and an NSERC Canada Graduate Scholarship for his doctoral research.

• • •